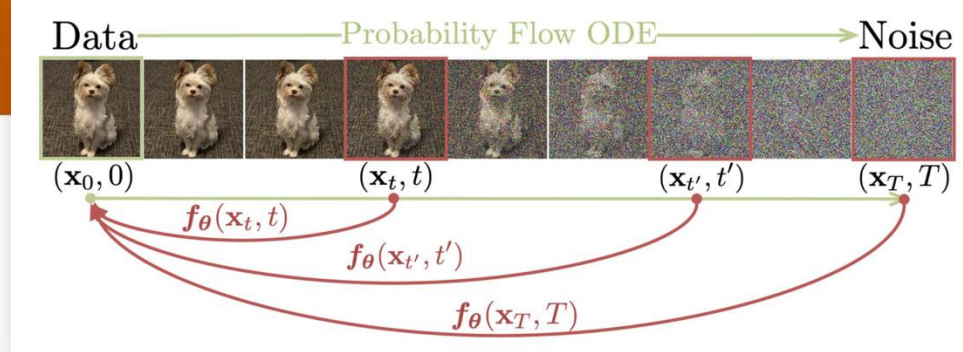


Continuous-Time Consistency Models

Guande He
2024.11.18

The Curse of Consistency



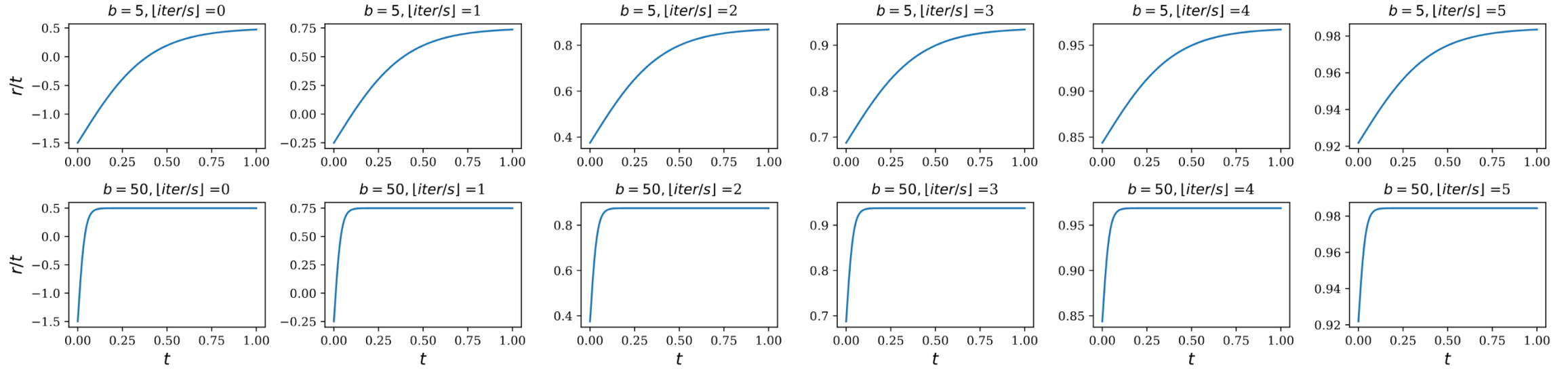
- From an optimization perspective, it's hard to deal with when $\Delta t \rightarrow 0$ due to error accumulation:

$$\|\mathbf{f}_\theta(\mathbf{x}_T) - \mathbf{x}_0\| \leq \sum_{i=1}^{N-1} \|\mathbf{f}_\theta(\mathbf{x}_{t_{i+1}}) - \mathbf{f}_\theta(\mathbf{x}_{t_i})\| \leq N e_{\max}$$

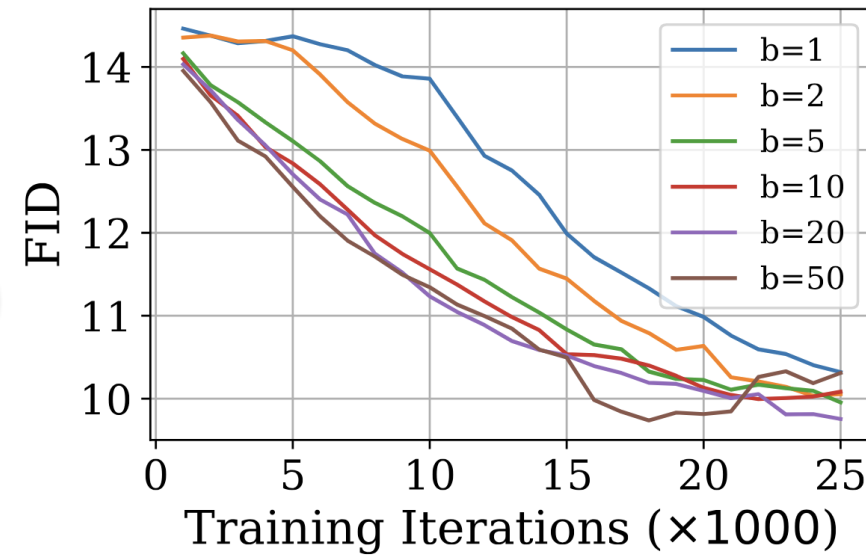
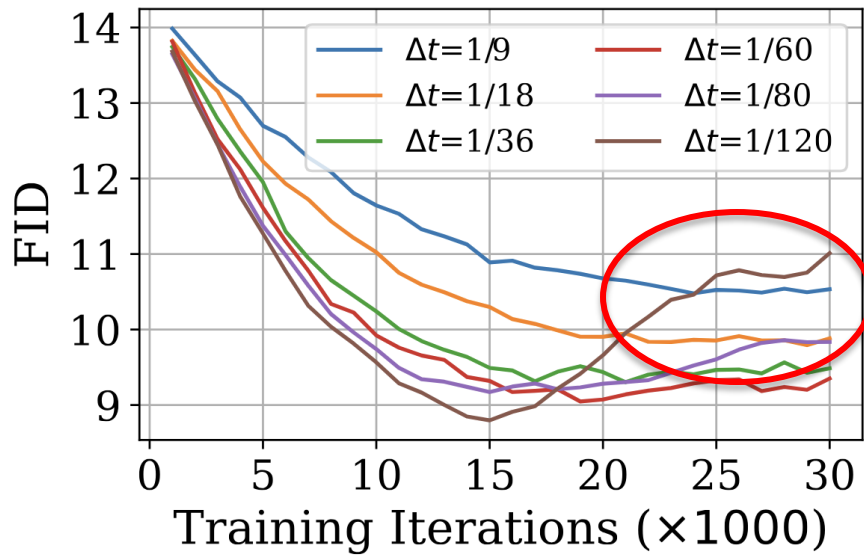
- This $\Delta t \rightarrow 0$ condition is **required** to guarantee the correctness of the “data score” used in consistency training, i.e., the marginal score is estimated with:

$$\nabla_{\mathbf{x}_t} \log p_t(\mathbf{x}_t) = -\mathbb{E} \left[\frac{\mathbf{x}_t - \alpha_t \mathbf{x}_t}{\sigma_t^2} \mid \mathbf{x}_t \right] \approx \frac{\mathbf{x}_t - \alpha_t \mathbf{x}_t}{\sigma_t^2}$$

- An expedient treatment is to manually design a “time step schedule” to gradually “shrink” Δt .
 - 🤔 But...



• An e
"shri



consistency

dually

Continuous-Time Consistency Models

- What happens to the objective when $\Delta t \rightarrow 0$? (From finite-difference to differential)

- Recall Consistency Distillation (in L2 distance, VE noise schedule):

$$\mathcal{L}_{\text{CD}}^N(\boldsymbol{\theta}, \boldsymbol{\theta}; \phi) := \mathbb{E}[\lambda(t_n) \|\mathbf{f}_{\boldsymbol{\theta}}(\mathbf{x}_{t_{n+1}}, t_{n+1}) - \mathbf{f}_{\boldsymbol{\theta}}(\hat{\mathbf{x}}_{t_n}^{\phi}, t_n)\|_2^2]$$

- We have $\lim_{N \rightarrow \infty} (N-1)^2 \mathcal{L}_{\text{CD}}^N(\boldsymbol{\theta}, \boldsymbol{\theta}; \phi) = \mathcal{L}_{\text{CD}}^{\infty}(\boldsymbol{\theta}, \boldsymbol{\theta}; \phi)$, where:

$$\mathcal{L}_{\text{CD}}^{\infty}(\boldsymbol{\theta}, \boldsymbol{\theta}; \phi) := \mathbb{E}\left[\frac{\lambda(t)}{[(\tau^{-1})'(t)]^2} \left\| \frac{\partial \mathbf{f}_{\boldsymbol{\theta}}(\mathbf{x}_t, t)}{\partial t} - t \frac{\partial \mathbf{f}_{\boldsymbol{\theta}}(\mathbf{x}_t, t)}{\mathbf{x}_t} \mathbf{s}_{\phi}(\mathbf{x}_t, t) \right\|_2^2\right]$$

- This is intuitive since

$$\begin{aligned} \mathbf{f}_{\boldsymbol{\theta}}(\mathbf{x}_t, t) &\equiv \mathbf{x}_{\epsilon} && \xrightarrow{\text{consistency condition}} \\ \iff \frac{\partial \mathbf{f}_{\boldsymbol{\theta}}(\mathbf{x}_t, t)}{\partial \mathbf{x}_t} \frac{d\mathbf{x}_t}{dt} + \frac{\partial \mathbf{f}_{\boldsymbol{\theta}}(\mathbf{x}_t, t)}{\partial t} &\equiv 0 \\ \iff \frac{\partial \mathbf{f}_{\boldsymbol{\theta}}(\mathbf{x}_t, t)}{\partial \mathbf{x}_t} [-t \mathbf{s}_{\phi}(\mathbf{x}_t, t)] + \frac{\partial \mathbf{f}_{\boldsymbol{\theta}}(\mathbf{x}_t, t)}{\partial t} &\equiv 0 && \text{(VE noise schedule)} \\ \iff \frac{\partial \mathbf{f}_{\boldsymbol{\theta}}(\mathbf{x}_t, t)}{\partial t} - t \frac{\partial \mathbf{f}_{\boldsymbol{\theta}}(\mathbf{x}_t, t)}{\partial \mathbf{x}_t} \mathbf{s}_{\phi}(\mathbf{x}_t, t) &\equiv 0. \end{aligned}$$

Continuous-Time Consistency Models

- The practice on discrete-time CMs suggests that using $\mathcal{L}_{\text{CD}}^N(\boldsymbol{\theta}, \text{sg}[\boldsymbol{\theta}]; \phi)$ instead of $\mathcal{L}_{\text{CD}}^N(\boldsymbol{\theta}, \boldsymbol{\theta}; \phi)$ stabilizes training.
- For continuous-time CM (in L2 distance, VE noise schedule):

$$\mathcal{L}_{\text{CD}}^{\infty}(\boldsymbol{\theta}, \boldsymbol{\theta}; \phi) := \mathbb{E} \left[\frac{\lambda(t)}{[(\tau^{-1})'(t)]^2} \left\| \frac{\partial \mathbf{f}_{\boldsymbol{\theta}}(\mathbf{x}_t, t)}{\partial t} - t \frac{\partial \mathbf{f}_{\boldsymbol{\theta}}(\mathbf{x}_t, t)}{\partial \mathbf{x}_t} s_{\phi}(\mathbf{x}_t, t) \right\|_2^2 \right]$$

$$\mathcal{L}_{\text{CD}}^{\infty}(\boldsymbol{\theta}, \text{sg}[\boldsymbol{\theta}]; \phi) := 2\mathbb{E} \left[\frac{\lambda(t)}{[(\tau^{-1})'(t)]^2} \mathbf{f}_{\boldsymbol{\theta}}(\mathbf{x}_t, t)^{\top} \left(\frac{\partial \mathbf{f}_{\text{sg}[\boldsymbol{\theta}]}(\mathbf{x}_t, t)}{\partial t} - t \frac{\partial \mathbf{f}_{\text{sg}[\boldsymbol{\theta}]}(\mathbf{x}_t, t)}{\partial \mathbf{x}_t} s_{\phi}(\mathbf{x}_t, t) \right) \right]$$

$$\mathcal{L}_{\text{CT}}^{\infty}(\boldsymbol{\theta}, \text{sg}[\boldsymbol{\theta}]) := 2\mathbb{E} \left[\frac{\lambda(t)}{[(\tau^{-1})'(t)]^2} \mathbf{f}_{\boldsymbol{\theta}}(\mathbf{x}_t, t)^{\top} \left(\frac{\partial \mathbf{f}_{\text{sg}[\boldsymbol{\theta}]}(\mathbf{x}_t, t)}{\partial t} - t \frac{\partial \mathbf{f}_{\text{sg}[\boldsymbol{\theta}]}(\mathbf{x}_t, t)}{\partial \mathbf{x}_t} \cdot \frac{\mathbf{x}_t - \mathbf{x}}{t} \right) \right]$$

- Asymptotic behavior:

No stop gradient version:

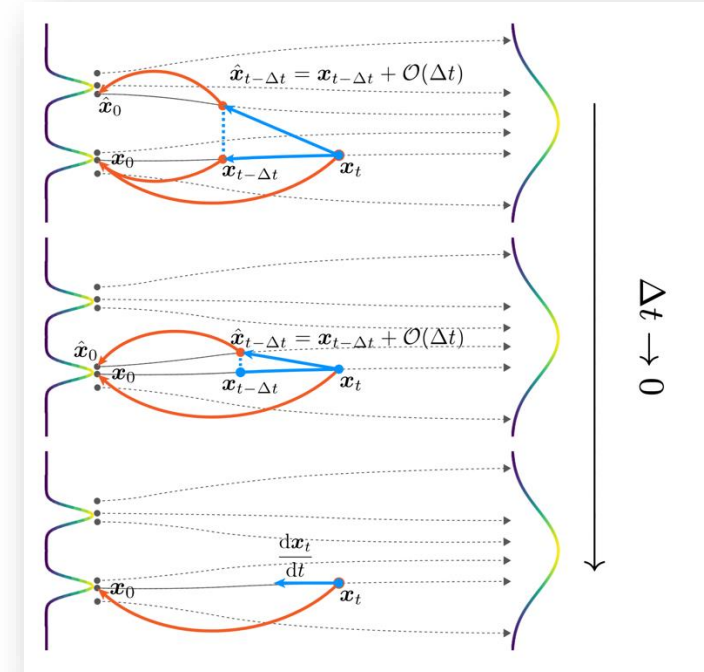
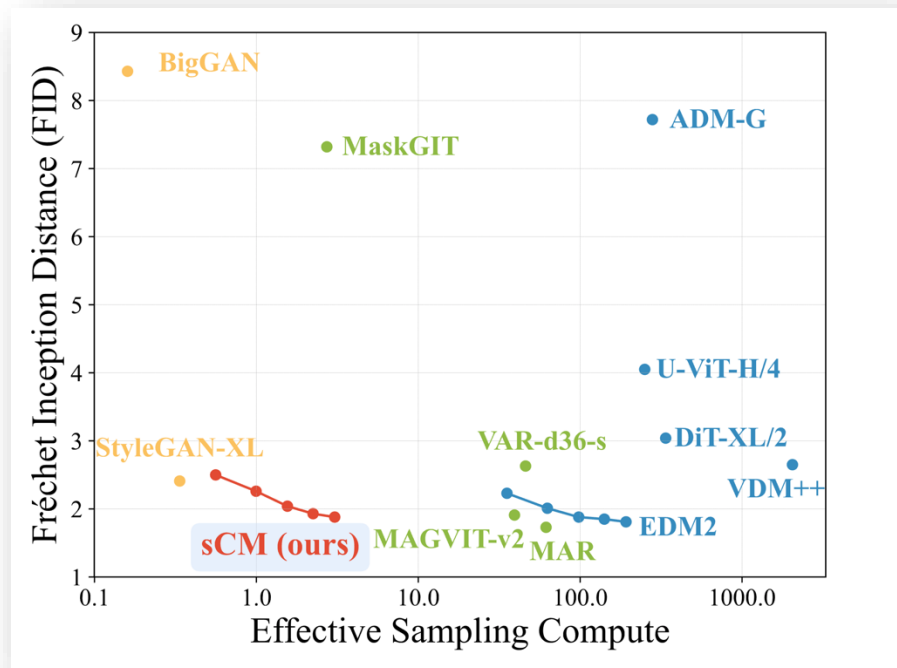
$$\lim_{N \rightarrow \infty} (N-1)^2 \mathcal{L}_{\text{CD}}^N(\boldsymbol{\theta}, \boldsymbol{\theta}; \phi) = \mathcal{L}_{\text{CD}}^{\infty}(\boldsymbol{\theta}, \boldsymbol{\theta}; \phi)$$

Stop gradient version:

$$\begin{aligned} \lim_{N \rightarrow \infty} (N-1)^2 \nabla_{\boldsymbol{\theta}} \mathcal{L}_{\text{CD}}^N(\boldsymbol{\theta}, \text{sg}[\boldsymbol{\theta}]; \phi) &= \nabla_{\boldsymbol{\theta}} \mathcal{L}_{\text{CD}}^{\infty}(\boldsymbol{\theta}, \text{sg}[\boldsymbol{\theta}]; \phi) \\ &= \lim_{N \rightarrow \infty} (N-1)^2 \nabla_{\boldsymbol{\theta}} \mathcal{L}_{\text{CT}}^N(\boldsymbol{\theta}, \text{sg}[\boldsymbol{\theta}]) = \nabla_{\boldsymbol{\theta}} \mathcal{L}_{\text{CT}}^{\infty}(\boldsymbol{\theta}, \text{sg}[\boldsymbol{\theta}]) \end{aligned}$$

Continuous-Time CMs can work!

- Although the continuous-time CM formulation is proposed on early 2023, there is no empirical practice successfully showing its effectiveness until Oct. 2024.
 - Developing empirical & engineering techniques tailored for the continuous-time CM objective!



Noise Schedule, Model Parameterization & Network Preconditioning (Empirical Design Space)

- Forward process / interpolation:

$$\mathbf{x}_t = \cos(t)\mathbf{x}_0 + \sin(t)\mathbf{z}, \quad \mathbf{x}_0 \sim p_d(\mathbf{x}_0), \mathbf{z} \sim \mathcal{N}(\mathbf{0}, \sigma_d^2 \mathbf{I}), t \in [0, \frac{\pi}{2}]$$

- The diffusion model (i.e., the velocity field in Rectified Flow) is parameterized as:

$$\mathbf{v}_\theta(\mathbf{x}_t, t) = \sigma_d \mathbf{F}_\theta(\mathbf{x}_t / \sigma_d, c_{\text{noise}}(t))$$

where \mathbf{F}_θ is a neural network. The PF-ODE is given by: $\frac{d\mathbf{x}_t}{dt} = \sigma_d \mathbf{F}_\theta \left(\frac{\mathbf{x}_t}{\sigma_d}, c_{\text{noise}}(t) \right)$

- Parameterization of consistency function:

$$\mathbf{f}_\theta(\mathbf{x}_t, t) = \cos(t)\mathbf{x}_t - \sin(t)\sigma_d \mathbf{F}_\theta \left(\frac{\mathbf{x}_t}{\sigma_d}, c_{\text{noise}}(t) \right)$$

- Insight here: using the DDIM-style first-order ODE discretization will automatically enforce the boundary condition $\mathbf{f}_\theta(\mathbf{x}_0, 0) \equiv \mathbf{0}$.
- Note: \mathbf{f}_θ is proportional to $\sin(t)\mathbf{F}_\theta$.

Stabilizing Continuous-time CMs

$$\frac{d\mathbf{f}_{\theta}(\mathbf{x}_t, t)}{dt} = \frac{\partial \mathbf{f}_{\theta}(\mathbf{x}_t, t)}{\partial \mathbf{x}_t} \frac{d\mathbf{x}_t}{dt} + \frac{\partial \mathbf{f}_{\theta}(\mathbf{x}_t, t)}{\partial t} \equiv 0$$

- Consider the “consistency condition” (tangent) term under the proposed design:

$$\frac{d\mathbf{f}_{\theta^-}}{dt} = -\cos(t) \left(\sigma_d \mathbf{F}_{\theta^-} \left(\frac{\mathbf{x}_t}{\sigma_d} \right) - \frac{d\mathbf{x}_t}{dt} \right) - \sin(t) \left(\mathbf{x}_t + \sigma_d \frac{d\mathbf{F}_{\theta^-}(\frac{\mathbf{x}_t}{\sigma_d}, t)}{dt} \right), \quad \theta^- := \text{sg}[\theta]$$

- The instability mainly comes from the scaled time derivative of the neural network $\sin(t) \partial_t \mathbf{F}_{\theta^-}$:

$$\sin(t) \partial_t \mathbf{F}_{\theta^-} = \sin(t) \frac{\partial c_{\text{noise}}(t)}{\partial t} \cdot \frac{\partial \text{emb}(c_{\text{noise}})}{\partial c_{\text{noise}}} \cdot \frac{\partial \mathbf{F}_{\theta^-}}{\partial \text{emb}(c_{\text{noise}})}$$

- Proposed treatment:

- Identity Time Transformation: $c_{\text{noise}}(t) = t$
- Re-design time embeddings $\text{emb}(c)$ with smaller gradient magnitudes.

- Adaptative Double Normalization Layer:

$$\mathbf{y} = \text{norm}(\mathbf{x}) \odot \text{pnorm}(\mathbf{s}(t)) + \text{pnorm}(b(t))$$

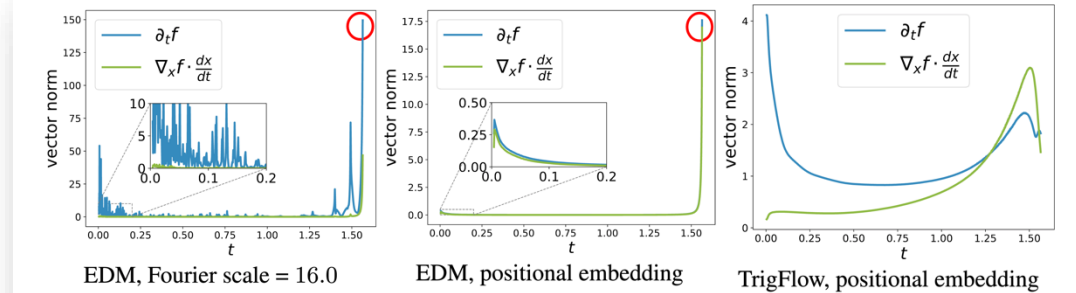


Figure 4: **Stability of different formulations.** We show the norms of both terms in $\frac{d\mathbf{f}_{\theta^-}}{dt} = \nabla_{\mathbf{x}} \mathbf{f}_{\theta^-} \cdot \frac{d\mathbf{x}_t}{dt} + \partial_t \mathbf{f}_{\theta^-}$ for diffusion models trained with the EDM ($c_{\text{noise}}(t) = \log(\sigma_d \tan(t))$) and TrigFlow ($c_{\text{noise}}(t) = t$) formulations using different time embeddings. We observe that large Fourier scales in Fourier embeddings cause instabilities. In addition, the EDM formulation suffers from numerical issues when $t \rightarrow \frac{\pi}{2}$, while TrigFlow (using positional embeddings) has stable partial derivatives for both \mathbf{x}_t and t .

Stabilizing Continuous-time CMs

• Tangent Normalization

- Explicitly normalizing $\frac{d\mathbf{f}_{\theta-}}{dt}$ with $\frac{d\mathbf{f}_{\theta-}}{dt} / \left(\left\| \frac{d\mathbf{f}_{\theta-}}{dt} \right\| + c \right)$
- Clipping $\frac{d\mathbf{f}_{\theta-}}{dt}$ within $[-1, 1]$.

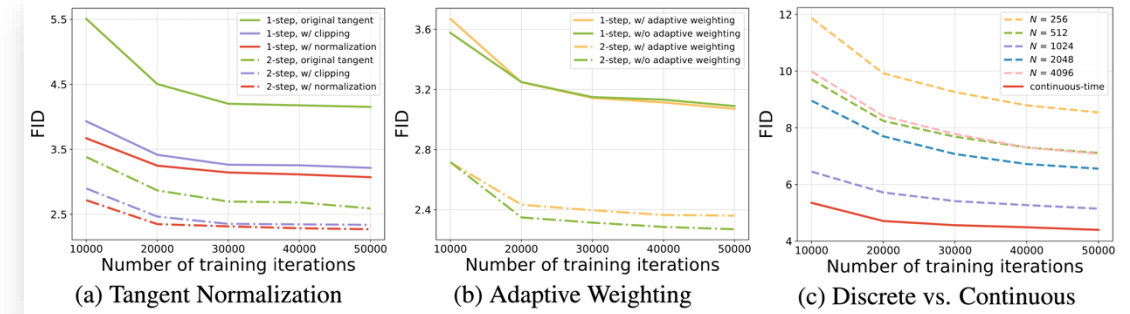
• Loss Trick & Adaptive Weighting

- Convert $\mathcal{L}_{\text{CM}}^{\infty}$ into a MSE loss using the trick $\nabla_{\theta} \mathbb{E}[\mathbf{F}_{\theta}^{\top} \mathbf{y}] = \frac{1}{2} \nabla_{\theta} \mathbb{E}[\|\mathbf{F}_{\theta} - \mathbf{F}_{\text{sg}[\theta]} + \mathbf{y}\|_2^2]$.
- Learn adaptive loss weighting during training:

$$\mathcal{L}_{\text{sCM}}(\theta, \phi) := \mathbb{E}_{\mathbf{x}_t, t} \left[\frac{e^{\omega_{\phi}(t)}}{D_{\mathbf{x}_0}} \left\| \mathbf{F}_{\theta} \left(\frac{\mathbf{x}_t}{\sigma_d}, t \right) - \mathbf{F}_{\theta-} \left(\frac{\mathbf{x}_t}{\sigma_d}, t \right) - \cos(t) \frac{d\mathbf{f}_{\theta-}(\mathbf{x}_t, t)}{dt} \right\|_2^2 - \omega_{\phi}(t) \right]$$

• Diffusion Fine-tuning & Tangent Warmup

- Fine-tuning from pre-trained diffusion models instead of training of scratch.
- Warm up the instable term $\sin(t)(\mathbf{x}_t + \sigma_d \frac{d\mathbf{F}_{\theta-}}{dt})$ by using $r \cdot \sin(t)$, r increases linearly from 0 to 1 over the first 100k training iterations.



Efficient Jacobian-Vector Product (JVP) Computation

- JVP Rearrangement**

- Vanilla calculation of $\frac{d\mathbf{F}_{\theta-}}{dt} = \nabla_{\mathbf{x}_t} \mathbf{F}_{\theta-} \cdot \frac{d\mathbf{x}_t}{dt} + \partial_t \mathbf{F}_{\theta-}$ using JVP of $\mathbf{F}_{\theta-}(\frac{\cdot}{\sigma_d}, \cdot)$ with input (\mathbf{x}_t, t) and tangent vector $(\frac{d\mathbf{x}_t}{dt}, 1)$ is prone to overflow.

- Using the fact that \mathbf{f}_{θ} is proportional to $\sin(t) \mathbf{F}_{\theta}$ and the sCM loss calculates $\cos(t) \frac{d\mathbf{f}_{\theta-}(\mathbf{x}_t, t)}{dt}$, the JVP can be implemented as:

$$\cos(t) \sin(t) \frac{d\mathbf{F}_{\theta-}}{dt} = \left(\nabla_{\frac{\mathbf{x}_t}{\sigma_d}} \mathbf{F}_{\theta-} \right) \cdot \left(\cos(t) \sin(t) \frac{d\mathbf{x}_t}{dt} \right) + \partial_t \mathbf{F}_{\theta-} \cdot (\cos(t) \sin(t) \sigma_d)$$

which is the JVP of $\mathbf{F}_{\theta-}(\cdot, \cdot)$ with input $(\frac{\mathbf{x}_t}{\sigma_d}, t)$ with tangent vector $(\cos(t) \sin(t) \frac{d\mathbf{x}_t}{dt}, \cos(t) \sin(t) \sigma_d)$

- The authors also modifies the Flash Attention to simultaneously compute softmax self-attention and its JVP in a single forward pass.

Benchmark Results

Table 1: Sample quality on unconditional CIFAR-10 and class-conditional ImageNet 64× 64.

Unconditional CIFAR-10			Class-Conditional ImageNet 64×64		
METHOD	NFE (↓)	FID (↓)	METHOD	NFE (↓)	FID (↓)
Diffusion models & Fast Samplers			Diffusion models & Fast Samplers		
Score SDE (deep) (Song et al., 2021b)	2000	2.20	ADM (Dhariwal & Nichol, 2021)	250	2.07
EDM (Karras et al., 2022)	35	2.01	RIN (Jabri et al., 2022)	1000	1.23
Flow Matching (Lipman et al., 2022)	142	6.35	DPM-Solver (Lu et al., 2022a)	20	3.42
DPM-Solver (Lu et al., 2022a)	10	4.70	EDM (Heun) (Karras et al., 2022)	79	2.44
DPM-Solver++ (Lu et al., 2022b)	10	2.91	EDM2 (Heun) (Karras et al., 2024)	63	1.33
DPM-Solver-v3 (Zheng et al., 2023c)	10	2.51			
Joint Training			Joint Training		
Diffusion GAN (Xiao et al., 2022)	4	3.75	StyleGAN-XL (Sauer et al., 2022)	1	1.52
Diffusion StyleGAN (Wang et al., 2022)	1	3.19	Diff-Instruct (Luo et al., 2024)	1	5.57
StyleGAN-XL (Sauer et al., 2022)	1	1.52	EMD (Xie et al., 2024b)	1	2.20
CTM (Kim et al., 2023)	1	1.87	DMD (Yin et al., 2024b)	1	2.62
Diff-Instruct (Luo et al., 2024)	1	4.53	DMD2 (Yin et al., 2024a)	1	1.28
DMD (Yin et al., 2024b)	1	3.77	SiD (Zhou et al., 2024)	1	1.52
SiD (Zhou et al., 2024)	1	1.92	CTM (Kim et al., 2023)	1	1.92
Diffusion Distillation			Moment Matching (Salimans et al., 2024)	1	3.00
DFNO (LPIPS) (Zheng et al., 2023b)	1	3.78		2	3.86
2-Rectified Flow (Liu et al., 2022)	1	4.85	Diffusion Distillation		
PID (LPIPS) (Tee et al., 2024)	1	3.92	DFNO (LPIPS) (Zheng et al., 2023b)	1	7.83
BOOT (LPIPS) (Gu et al., 2023)	1	4.38	PID (LPIPS) (Tee et al., 2024)	1	9.49
Consistency-FM (Yang et al., 2024)	2	5.34	TRACT (Berthelot et al., 2023)	1	7.43
PD (Salimans & Ho, 2022)	1	8.34		2	4.97
	2	5.58	PD (Salimans & Ho, 2022)	1	10.70
	2	3.32	(reimpl. from Heek et al. (2024))	2	4.70
TRACT (Berthelot et al., 2023)	1	3.78	CD (LPIPS) (Song et al., 2023)	1	6.20
	2	2.93		2	4.70
CD (LPIPS) (Song et al., 2023)	1	3.55	MultiStep-CD (Heek et al., 2024)	1	3.20
	2	2.93		2	1.90
sCD (ours)	1	3.66	sCD (ours)	1	2.44
	2	2.52		2	1.66
Consistency Training			Consistency Training		
iCT (Song & Dhariwal, 2023)	1	2.83	iCT (Song & Dhariwal, 2023)	1	4.02
	2	2.46		2	3.20
iCT-deep (Song & Dhariwal, 2023)	1	2.51	iCT-deep (Song & Dhariwal, 2023)	1	3.25
	2	2.24		2	2.77
ECT (Geng et al., 2024)	1	3.60	ECT (Geng et al., 2024)	1	2.49
	2	2.11		2	1.67
sCT (ours)	1	2.97	sCT (ours)	1	2.04
	2	2.06		2	1.48

 Table 2: Sample quality on class-conditional ImageNet 512× 512. [†]Our reimplemented teacher diffusion model based on EDM2 (Karras et al., 2024) but with modifications in Sec. 4.1.

METHOD	NFE (↓)	FID (↓)	#Params	METHOD	NFE (↓)	FID (↓)	#Params
Diffusion models				Teacher Diffusion Model			
ADM-G (Dhariwal & Nichol, 2021)	250×2	7.72	559M	EDM2-S (Karras et al., 2024)	63×2	2.29	280M
RIN (Jabri et al., 2022)	1000	3.95	320M	EDM2-M (Karras et al., 2024)	63×2	2.00	498M
U-ViT-H/4 (Bao et al., 2023)	250×2	4.05	501M	EDM2-L (Karras et al., 2024)	63×2	1.87	778M
DiT-XL/2 (Peebles & Xie, 2023)	250×2	3.04	675M	EDM2-XL (Karras et al., 2024)	63×2	1.80	1.1B
SimDiff (Hooeboom et al., 2023)	512×2	3.02	2B	EDM2-XXL (Karras et al., 2024)	63×2	1.73	1.5B
VDM++ (Kingma & Gao, 2024)	512×2	2.65	2B	Consistency Training (sCT, ours)			
DiffT (Hatamizadeh et al., 2023)	250×2	2.67	561M	sCT-S (ours)	1	10.13	280M
DiMR-XL/3R (Liu et al., 2024)	250×2	2.89	525M		2	9.86	280M
DiffUSM-XL (Yan et al., 2024)	250×2	3.41	673M	sCT-M (ours)	1	5.84	498M
DiM-H (Teng et al., 2024)	250×2	3.78	860M		2	5.53	498M
U-DiT (Tian et al., 2024b)	250	15.39	204M	sCT-L (ours)	1	5.15	778M
SiT-XL (Ma et al., 2024)	250×2	2.62	675M		2	4.65	778M
Large-DiT (Alpha-VLLM, 2024)	250×2	2.52	3B	sCT-XL (ours)	1	4.33	1.1B
MaskDiT (Zheng et al., 2023a)	79×2	2.50	736M		2	3.73	1.1B
DiS-H/2 (Fei et al., 2024a)	250×2	2.88	900M	sCT-XXL (ours)	1	4.29	1.5B
DRWKV-H/2 (Fei et al., 2024b)	250×2	2.95	779M		2	3.76	1.5B
EDM2-S (Karras et al., 2024)	63×2	2.23	280M	Consistency Distillation (sCD, ours)			
EDM2-M (Karras et al., 2024)	63×2	2.01	498M	sCD-S	1	3.07	280M
EDM2-L (Karras et al., 2024)	63×2	1.88	778M		2	2.50	280M
EDM2-XL (Karras et al., 2024)	63×2	1.85	1.1B	sCD-M	1	2.75	498M
EDM2-XXL (Karras et al., 2024)	63×2	1.81	1.5B		2	2.26	498M
GANs & Masked Models				sCD-L	1	2.55	778M
BigGAN (Brock, 2018)	1	8.43	160M		2	2.04	778M
StyleGAN-XL (Sauer et al., 2022)	1×2	2.41	168M	sCD-XL	1	2.40	1.1B
VQGAN (Esser et al., 2021)	1024	26.52	227M		2	1.93	1.1B
MaskGIT (Chang et al., 2022)	12	7.32	227M	sCD-XXL	1	2.28	1.5B
MAGVIT-v2 (Yu et al., 2023)	64×2	1.91	307M		2	1.88	1.5B
MAR (Li et al., 2024)	64×2	1.73	481M				
VAR-d36-s (Tian et al., 2024a)	10×2	2.63	2.3B				

Scalability & Sample Diversity

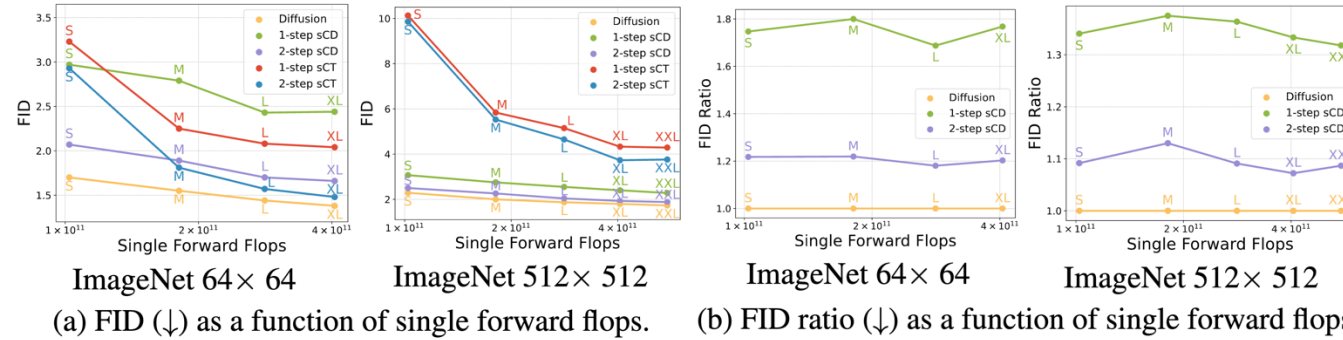


Figure 6: **sCD scales commensurately with teacher diffusion models.** We plot the (a) FID and (b) FID ratio against the teacher diffusion model (at the same model size) on ImageNet 64×64 and 512×512. sCD scales better than sCT, and has a *constant offset* in the FID ratio across all model sizes, implying that sCD has the same scaling property of the teacher diffusion model. Furthermore, the offset diminishes with more sampling steps.

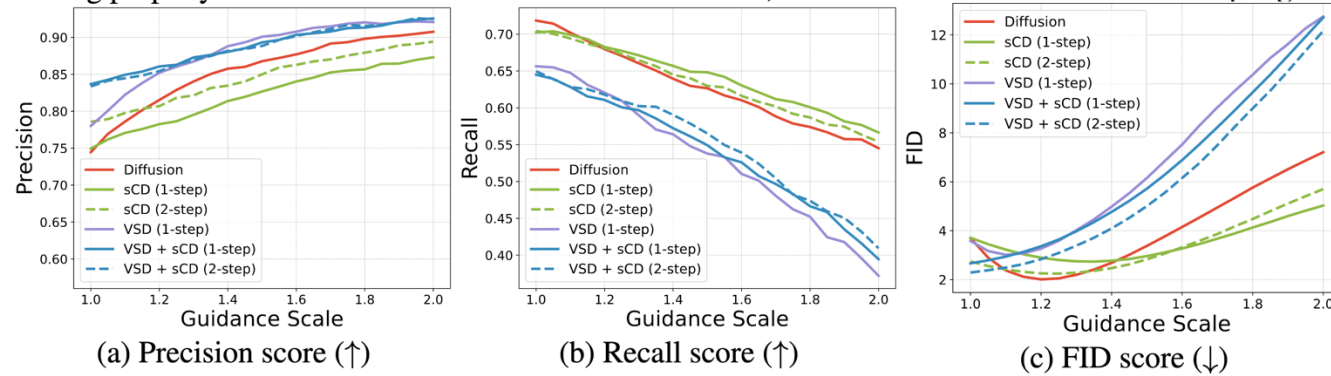


Figure 7: **sCD has higher diversity compared to VSD:** Sample quality comparison of the EDM2 (Karras et al., 2024) diffusion model, VSD (Wang et al., 2024; Yin et al., 2024b), sCD, and the combination of VSD and sCD, across varying guidance scales. All models are of EDM2-M size and trained on ImageNet 512×512.

Thanks!